



The particle–fluid–particle pressure tensor for ideal-fluid–particle flow

Rodney O. Fox^{1,2}

¹Department of Chemical and Biological Engineering, Iowa State University, 618 Bissell Road, Ames, IA 50011-1098, USA

²Center for Multiphase Flow Research and Education, Iowa State University, Ames, IA, USA

Corresponding author: Rodney O. Fox, rofox@iastate.edu

(Received 3 February 2025; revised 19 March 2025; accepted 19 March 2025)

Starting from the coupled Boltzmann–Enskog (BE) kinetic equations for a two-particle system consisting of hard spheres, a hyperbolic two-fluid model for binary, hard-sphere mixtures was derived in Fox (2019, *J. Fluid Mech.* **877**, 282). In addition to spatial transport, the BE kinetic equations account for particle–particle collisions, using an elastic hard-sphere collision model, and the Archimedes (buoyancy) force due to spatial gradients of the pressure in each phase, as well as other forces involving spatial gradients. The ideal-fluid–particle limit of this model is found by letting one of the particle diameters go to zero while the other remains finite. The resulting two-fluid model has closed terms for the spatial fluxes and momentum exchange due to the excluded volume occupied by the particles, e.g. a momentum-exchange term \mathbf{F}_{fp} that depends on gradients of the fluid density ρ_f , fluid velocity \mathbf{u}_f and fluid pressure p_f . In Zhang *et al.* (2006, *Phy. Rev. Lett.* **97**, 048301), the corresponding unclosed momentum-exchange term depends on the divergence of an unknown particle–fluid–particle (pfp) stress (or pressure) tensor. Here, it is shown that the pfp-pressure tensor \mathbf{P}_{pfp} can be found in closed form from the expression for \mathbf{F}_{fp} derived in Fox (2019, *J. Fluid Mech.* **877**, 282). Remarkably, using this expression for \mathbf{P}_{pfp} ensures that the two-fluid model for ideal-fluid–particle flow is well posed for all fluid-to-particle material-density ratios $Z = \rho_f / \rho_p$.

Key words: particle/fluid flow, kinetic theory

1. Introduction

Despite the fact that such models are most often ill posed (Lhuillier, Chang & Theofanous 2013), two-fluid models have found widespread use for simulating industrial

and environmental polydisperse multiphase flows (Fox 2024). The principal modelling difficulty to achieving a well-posed system results from the Archimedes force, involving the continuous fluid pressure gradient, for cases where the particle-phase material density ρ_p is smaller than that of the fluid ρ_f (Lhuillier *et al.* 2013). In addition to being non-physical, ill-posed two-fluid models suffer from numerical instabilities due to complex eigenvalues, yielding spurious oscillations (Panicker, Passalacqua & Fox 2018). Given that two-fluid models are usually derived from well-posed microscale models (e.g. the Navier–Stokes equation for the fluid phase coupled to Newton’s equations for the particles) (Drew & Passman 1998; Zhang, Ma & Rauenzahn 2006), it is clear that they are ill posed due to the approximations used to close the model equations. In general, there are two types of unclosed terms: (i) terms modifying the spatial fluxes of mass, momentum and energy; and (ii) source terms for exchange of mass, momentum and energy. For example, in the volume-averaging approach (Drew & Passman 1998), the source terms for momentum and energy exchange involve unclosed particle-surface integrals depending on the fluid stresses at the particle surface. Similarly, in the kinetic approach of Zhang *et al.* (2006) an unclosed particle–fluid–particle (pfp) stress tensor Σ_{pfp} arises from fluid-mediated (or hydrodynamic) forces on a given particle due to the surrounding particles (see Wang *et al.* 2021; Zhang 2021 for more details).

With these difficulties in mind, Fox (2019) derived a two-fluid model for ideal-fluid–particle flow starting from the Boltzmann–Enskog (BE) kinetic equation for hard spheres with disparate sizes. As done in the derivation of the Euler equations for gas dynamics (Cercignani 1988), the goal was to find exact expressions for the fluxes and source terms in the two-fluid model for a specific system with well-defined interactions between the phases (i.e. binary, hard-sphere collisions). Such a model can then be analysed to check if it is well posed and, if so, to determine what are the necessary properties of the fluxes and source terms. As is well known, the (inviscid) Euler equations for an ideal fluid can be found from the Boltzmann kinetic equation for monodisperse hard spheres. For a binary system of hard spheres with different diameters $d_1 \ll d_2$, the BE kinetic equation is used to model how spatial gradients in the macroscopic variables (e.g. density, velocity, pressure) affect the collision rates between particles with different diameters (Chapman & Cowling 1952). For example, in order to include the Archimedes force in the momentum balances, the binary collision operators in the BE kinetic equation require a specific form for the particle-pair distribution function (see Fox 2019 and § 2 for details). In addition to the Archimedes force, this distribution function generates a momentum-exchange term (denoted by $F_{fp} = -F_{pf}$) involving spatial gradients in the fluid-phase density ρ_f and the fluid-phase velocity \mathbf{u}_f . Likewise, the presence of particles modifies the momentum and energy fluxes in the fluid phase. For the binary hard-sphere system, it is in fact these additional terms that are responsible for making the two-fluid model well posed (see analysis in Fox 2019 and § 4) for material-density ratio $Z = \rho_f/\rho_p \leq 0.1$.

In order to make the two-fluid model well posed for arbitrary Z , Fox, Laurent & Vié (2020) included added mass as first proposed by Cook & Harlow (1984). In the kinetic equation, the definition of a particle was extended to include some fluid (i.e. the added mass) travelling with the velocity of the particle. The effective material density of a particle ρ_e is defined using the sum of the particle mass and the added mass. As a result, the material-density ratio ρ_f/ρ_e remains finite when $\rho_p \rightarrow 0$. Besides added mass, Fox *et al.* (2020) introduced an *ad hoc* model for the pfp-pressure tensor \mathbf{P}_{pfp} (or, equivalently, a model for $-\Sigma_{pfp}$). They justified this additional hydrodynamic stress by the fact that, when $Z \gg 1$ (e.g. bubbly flows), particle–particle interactions are strongly mediated by the fluid phase (Wang *et al.* 2021; Zhang 2021), as opposed to hard-sphere collisions. Nonetheless, while this augmented two-fluid model with added mass is well posed for

arbitrary Z , the question of what is the exact form for \mathbf{P}_{pfp} still remains. Indeed, the general analysis by Zhang *et al.* (2006) shows that the pfp-stress tensor should exist in any kinetic derivation of the two-fluid model. If this is true, then what is the exact expression for \mathbf{P}_{pfp} in the hard-sphere model of Fox (2019), and how is it related to \mathbf{F}_{fp} ? Answering these questions is the principal objective of this work.

The remainder of this article is organised as follows. In § 2, we briefly review the BE kinetic model with emphasis on the particle-pair distribution function in the ideal-fluid–particle limit. The two-fluid model derived in Fox (2019) for an ideal fluid and spherical particles is also provided in § 2. The main result concerning the relationship between \mathbf{F}_{fp} and \mathbf{P}_{pfp} is derived in § 3. Finally, in § 4, we find explicit expressions for the eigenvalues of the two-fluid model for a constant-density fluid, and discuss how the results from this work can be applied to the two-fluid models containing additional physics discussed in Fox (2024).

2. Boltzmann–Enskog kinetic model

In Fox (2019), a hyperbolic two-fluid model was derived, starting from the BE kinetic equation, that includes the Archimedes force. The derivation used binary, hard-sphere collisions for particles with diameters $d_1 \leq d_2$, and resulted in a two-fluid model for the limit $d_1 \ll d_2$, e.g. a molecular gas containing finite-size particles. In this section, we briefly review the principal assumptions and results for an ideal-fluid–particle flow.

2.1. Principal assumptions

For simplicity and clarity, we only consider the ideal-fluid case. The kinetic theory model in Fox (2019) uses the Enskog term for the two-particle distribution function at the contact point (i.e. on the surface of the particle with diameter d_p)

$$f^{(2)}(\mathbf{v}_f, \mathbf{v}_p) = f_f(\mathbf{v}_f) f_p(\mathbf{v}_p) + \frac{1}{2} d_p f_p(\mathbf{v}_p) \mathbf{x}_{12} \cdot \partial_{\mathbf{x}} f_f(\mathbf{v}_f), \quad (2.1)$$

where \mathbf{x}_{12} is the unit vector pointing from the surface contact point for collision with a fluid particle to the particle centre. The reader will recognise (2.1) as a Taylor-like expansion of the fluid-velocity distribution function (VDF), denoted by f_f , from the particle surface to its centre. The principal assumption used to derive the two-fluid model is that (2.1) is valid when spatial gradients are small enough to neglect higher-order terms.

Another assumption is that the VDF for an ideal fluid is Maxwellian

$$f_f(\mathbf{v}_f) = \frac{\rho_f(t, \mathbf{x})}{[2\pi \Theta_f(t, \mathbf{x})]^{3/2}} \exp\left(-\frac{|\mathbf{v}_f - \mathbf{u}_f(t, \mathbf{x})|^2}{2\Theta_f(t, \mathbf{x})}\right), \quad (2.2)$$

with velocity variance Θ_f and fluid pressure $p_f = \rho_f \Theta_f$. Notice that f_f depends on \mathbf{x} and t through three moments, e.g. fluid density ρ_f , fluid velocity \mathbf{u}_f and fluid pressure p_f (one could also use Θ_f in place of p_f , but p_f is more convenient for separating the Archimedes (buoyancy) force from the hydrodynamic force \mathbf{F}_{fp} . Θ_f is proportional to the thermodynamic temperature T_f .) and not explicitly. Thus, the Enskog term in (2.1) can be written using the following expression for the spatial gradient (summation over i):

$$\partial_{\mathbf{x}} f_f = \left(\frac{\partial f_f}{\partial \rho_f}\right) \partial_{\mathbf{x}} \rho_f + \left(\frac{\partial f_f}{\partial u_{f,i}}\right) \partial_{\mathbf{x}} u_{f,i} + \left(\frac{\partial f_f}{\partial p_f}\right) \partial_{\mathbf{x}} p_f. \quad (2.3)$$

On the right-hand side of (2.3), only the partial derivatives of f_f depend on \mathbf{v}_f through (2.2). In the kinetic theory model, the gradients of all hydrodynamic variables are considered, not just the pressure gradient needed for the Archimedes force.

Even before doing the detailed calculations to evaluate the collision integrals, we can already observe from (2.3) that the Archimedes force will come from the term involving $\partial_{\mathbf{x}} p_f$, while the two other terms generate \mathbf{F}_{pf} . In other words, \mathbf{F}_{pf} results from fluid density and velocity gradients across the particle radius. Note that the separation of $f^{(2)}$ into two contributions is done in a more general formulation by Zhang *et al.* (2006) and Zhang (2021). The interest of using (2.1) as a specific example is that it allows us to find an exact expression for \mathbf{F}_{pf} , valid when spatial gradients of f_f are small. In contrast, Wang *et al.* (2021) find an approximate correlation for \mathbf{F}_{pf} from particle-resolved DNS (direct-numerical simulation) that depends on particle-phase volume fraction α_p and the particle Reynolds number Re_p . Generally speaking, small Re_p is a sufficient condition for small spatial variation of f_f . Thus, the main assumption from which all the results below follow is that (2.1) is a physically relevant approximation for $f^{(2)}$.

2.2. Collision integrals with Maxwellian VDF

The collision integral that generates the force of an ideal fluid on a spherical particle of diameter d_p uses the approximation in (2.1) for $f^{(2)}$. The first term on the right-hand side ($f_f f_p$) is the Boltzmann closure, while the second accounts for variations of f_f around the particle surface. The latter is the Enskog closure that keeps only the first derivative in \mathbf{x} . As shown in Fox (2019), the fluid-drag force depends on the first term in (2.1), while the Archimedes and hydrodynamic forces depend on the second. For clarity, we shall also assume that the particle VDF is Maxwellian

$$f_p(\mathbf{v}_p) = \frac{\rho_p \alpha_p(t, \mathbf{x})}{[2\pi \Theta_p(t, \mathbf{x})]^{3/2}} \exp\left(-\frac{|\mathbf{v}_p - \mathbf{u}_p(t, \mathbf{x})|^2}{2\Theta_p(t, \mathbf{x})}\right), \tag{2.4}$$

and the particle–particle collisions are elastic. A more general form where the particle velocity variance (Θ_p is often referred to as granular temperature.) Θ_p is a tensor (i.e. anisotropic Gaussian) and the collisions are inelastic can be found in Fox (2019). Note that ρ_p is constant and the fluid-phase volume fraction is defined by $\alpha_f = 1 - \alpha_p$.

The specific forms of the collision integral can be found in Fox (2019). For momentum, the forms (explicitly showing the dependence on \mathbf{v}_f and \mathbf{v}_p) are the vector

$$C^{(0)} = \frac{3}{2\rho_p d_p} \int_{\mathbb{R}^6} (\mathbf{v}_f - \mathbf{v}_p) |\mathbf{v}_f - \mathbf{v}_p| f_f(\mathbf{v}_f) f_p(\mathbf{v}_p) d\mathbf{v}_f d\mathbf{v}_p, \tag{2.5}$$

and the vector $C^{(1)}$ with components

$$C_i^{(1)} = \frac{1}{5\rho_p} \sum_j \int_{\mathbb{R}^6} I_{i,j}(\mathbf{v}_f - \mathbf{v}_p) f_p(\mathbf{v}_p) \partial_{x_j} f_f(\mathbf{v}_f) d\mathbf{v}_f d\mathbf{v}_p, \tag{2.6}$$

where the symmetric second-order tensor $I_{i,j}$ has diagonal elements $I_{i,i}(\mathbf{v}) = \mathbf{v}^2 + 2v_i^2$ and off-diagonal elements $I_{i,j}(\mathbf{v}) = 2v_i v_j$ (i.e. $I_{i,j}(\mathbf{v}) = \mathbf{v}^2 \delta_{i,j} + 2v_i v_j$). This tensor is found by integration over the collision surface of a particle, and all such integrals have a closed form for integer velocity moments (see Fox 2019 for details). Notice that $I_{i,j}$ does not depend on \mathbf{x} or t , only on the independent variable \mathbf{v} . For a Maxwellian VDF, velocity moments of orders 0, 1 and 2 suffice to find the mass, momentum and total energy balances. The collision integrals for mass are null, and those for energy are given in Fox (2019). Here, we consider only (2.5) and (2.6) for momentum exchange.

2.2.1. Fluid-drag force

The parameter $C^{(0)}$ represents the drag force and the integral is unclosed due to $|\mathbf{v}_f - \mathbf{v}_p|$. For the ideal-fluid case, both f_f and f_p are Maxwellian. Approximating the integrals yields an expression for the drag coefficient K . In general, $\Theta_f \gg \Theta_p$ when Re_p is small so that $K \propto 6 \alpha_p \rho_f \Theta_f^{1/2} / d_p$. This approximation is inaccurate and higher-order terms in the VDF are required (see van Beijeren & Dorfman 1980a,b for details). In practice, K is found using a drag correlation (Capecelatro 2022).

2.2.2. Forces due to spatial gradients

The parameter $C^{(1)}$ represents all of the forces that depend on the spatial gradient $\partial_x f_f$. Substituting (2.3) leads to three separate contributions (summation over j)

$$\begin{aligned} & \left[\int_{\mathbb{R}^6} I_{i,j}(\mathbf{v}_f - \mathbf{v}_p) \left(\frac{\partial \ln f_f}{\partial \rho_f} \right) f_p(\mathbf{v}_p) f_f(\mathbf{v}_f) d\mathbf{v}_f d\mathbf{v}_p \right] \partial_{x_j} \rho_f \\ & \left[\int_{\mathbb{R}^6} I_{i,j}(\mathbf{v}_f - \mathbf{v}_p) \left(\frac{\partial \ln f_f}{\partial u_{f,k}} \right) f_p(\mathbf{v}_p) f_f(\mathbf{v}_f) d\mathbf{v}_f d\mathbf{v}_p \right] \partial_{x_j} u_{f,k} \\ & \left[\int_{\mathbb{R}^6} I_{i,j}(\mathbf{v}_f - \mathbf{v}_p) \left(\frac{\partial \ln f_f}{\partial p_f} \right) f_p(\mathbf{v}_p) f_f(\mathbf{v}_f) d\mathbf{v}_f d\mathbf{v}_p \right] \partial_{x_j} p_f, \end{aligned} \tag{2.7}$$

where (the integral $\int_{\mathbb{R}^3} |\mathbf{v}_f - \mathbf{u}_f|^2 f_f d\mathbf{v}_f$ (trace of velocity covariance) equals $3\rho_f \Theta_f = 3p_f$ and $\int_{\mathbb{R}^3} f_f d\mathbf{v}_f = \rho_f$. Gaussian moments of order higher than two have known dependencies of ρ_f , \mathbf{u}_f and Θ_f)

$$\begin{aligned} \frac{\partial \ln f_f}{\partial \rho_f} &= \frac{3}{2\rho_f} - \frac{|\mathbf{v}_f - \mathbf{u}_f|^2}{6p_f}, \quad \frac{\partial \ln f_f}{\partial \mathbf{u}_f} = \frac{\rho_f(\mathbf{v}_f - \mathbf{u}_f)}{p_f}, \\ \frac{\partial \ln f_f}{\partial p_f} &= -\frac{1}{2p_f} + \frac{\rho_f |\mathbf{v}_f - \mathbf{u}_f|^2}{6p_f^2}. \end{aligned} \tag{2.8}$$

An important technical point is that the three integrals in the square brackets in (2.7) are closed, i.e. they can be evaluated exactly and depend on ρ_f , \mathbf{u}_f , Θ_f and $\rho_p \alpha_p$, \mathbf{u}_p , Θ_p . (See Fox 2019 for details.) Remarkably, the integral multiplying $\partial_{x_j} p_f$ reduces to $\alpha_p \delta_{i,j}$, yielding the Archimedes force. The other two integrals yield (in Fox 2019, an equivalent procedure is used to find the Archimedes and hydrodynamic forces. Because $I_{i,j}$ does not depend on \mathbf{x} , the velocity integrals can be computed *before* taking the spatial derivatives of the fluid variables. This procedure reduces the number of integrals to evaluate from three to one, making it easier to extend to higher-order moments)

$$\mathbf{F}_{pf} = \alpha_p (\Theta_p \mathbf{I} + \mathbf{R}) \cdot \partial_x \rho_f + \rho_f \alpha_p \frac{2}{5} [\mathbf{u}_{fp} \cdot (\partial_x \mathbf{u}_f) + (\partial_x \mathbf{u}_f) \cdot \mathbf{u}_{fp} + (\partial_x \cdot \mathbf{u}_f) \mathbf{u}_{fp}], \tag{2.9}$$

where $\mathbf{u}_{fp} = \mathbf{u}_f - \mathbf{u}_p$ and

$$\mathbf{R} = \frac{1}{5} u_{fp}^2 \mathbf{I} + \frac{2}{5} \mathbf{u}_{fp} \otimes \mathbf{u}_{fp}, \tag{2.10}$$

with $tr(\mathbf{R}) = u_{fp}^2$. Note that, because here we separate out the term involving $\Theta_p \mathbf{I}$ when defining \mathbf{R} , this definition is slightly different than in Fox (2019).

In Fox (2019), the exact expression for $C^{(1)}$ for arbitrary VDFs (e.g. depending on the velocity covariance matrix, etc.) is computed. Thus, (2.9) represents the lowest-order approximation assuming Maxwellian VDFs. In any case, the accuracy of this result depends mainly on the accuracy of the model for $f^{(2)}$ in (2.1).

2.3. Two-fluid model for fluid–particle flow

For completeness, we provide the two-fluid model with an ideal fluid in table 1. Our main objective in the next section is to demonstrate that the momentum-exchange term F_{pf} in (2.9) provides a closed expression for the pfp-pressure tensor P_{pfp} introduced in an *ad hoc* manner in Fox *et al.* (2020). The tensor R results from integrating over the collision surface of a spherical particle (see chapter 6 in Marchisio & Fox 2013 for details). Notice that R appears in the fluid-phase momentum flux (‘collisional’ flux) in the momentum balance in table 1 (see Fox 2019 for details). This result is also found by volume averaging over the surface of spherical particles (Lhuillier 2023), and arises due to the excluded volume occupied by particles. This would suggest that the fluid-phase momentum flux in the two-fluid model with spherical particles should always depend on R , regardless of how it is derived.

3. Particle–fluid–particle pressure tensor

In this section, we show how to find a closed expression for the pfp-pressure tensor P_{pfp} from the momentum-exchange term F_{pf} in (2.9). The derivation of P_{pfp} requires us to express the gradient of the fluid velocity $\partial_x u_f$ in terms of the slip velocity u_{pf} and the volume-average velocity u_v defined by

$$u_v = \alpha_p u_p + \alpha_f u_f = \alpha_p u_{pf} + u_f. \tag{3.1}$$

From the mass balances in table 1, it can easily be shown that if the material densities (i.e. ρ_f and ρ_p) are constant, then $\partial_x \cdot u_v = 0$. Thus, u_v is the ‘natural’ choice for the reference velocity. The momentum-exchange terms in (2.9) can then be rewritten using the identity

$$\partial_x u_f = \partial_x u_v + \partial_x (\alpha_p u_{pf}). \tag{3.2}$$

In particular, by rearranging the terms on the left-hand side below (which appears in F_{fp}), we find that

$$\begin{aligned} & \rho_f \alpha_p \frac{2}{5} [u_{fp} \cdot (\partial_x u_f) + (\partial_x u_f) \cdot u_{fp} + (\partial_x \cdot u_f) u_{fp}] \\ &= \rho_f \alpha_p \frac{2}{5} [2\Gamma_v + (\partial_x \cdot u_v) I] \cdot u_{fp} + \rho_f \partial_x \cdot (\alpha_p^2 R), \end{aligned} \tag{3.3}$$

where $\Gamma_v = \frac{1}{2}[(\partial_x u_v) + (\partial_x u_v)^t]$ is the rate-of-deformation tensor for the volume-average velocity.

The pfp-pressure tensor is then defined by

$$P_{pfp} = \rho_f \alpha_p^2 R, \tag{3.4}$$

such that $\partial_x \cdot P_{pfp} = \rho_f \partial_x \cdot (\alpha_p^2 R) + \alpha_p^2 R \cdot \partial_x \rho_f$. The dependence of P_{pfp} on α_p^2 is consistent with it arising from particle-pair interactions, while the dependence on ρ_f shows the role of the fluid. Using these results, the momentum-exchange term becomes

Mass balances

$$\begin{aligned} \partial_t(\rho_f \alpha_f) + \partial_{\mathbf{x}} \cdot (\rho_f \alpha_f \mathbf{u}_f) &= 0 \\ \partial_t(\rho_p \alpha_p) + \partial_{\mathbf{x}} \cdot (\rho_p \alpha_p \mathbf{u}_p) &= 0 \end{aligned}$$

momentum balances

$$\begin{aligned} \rho_f \alpha_f (\partial_t + \mathbf{u}_f \cdot \partial_{\mathbf{x}}) \mathbf{u}_f + \partial_{\mathbf{x}} \cdot [\alpha_p \rho_f (\Theta_p \mathbf{I} + \mathbf{R})] + \alpha_f \partial_{\mathbf{x}} p_f &= \mathbf{F}_{pf} + K \mathbf{u}_{pf} + \rho_f \alpha_f \mathbf{g} \\ \rho_p \alpha_p (\partial_t + \mathbf{u}_p \cdot \partial_{\mathbf{x}}) \mathbf{u}_p + \partial_{\mathbf{x}} p_p + \alpha_p \partial_{\mathbf{x}} p_f &= \mathbf{F}_{fp} + K \mathbf{u}_{fp} + \rho_p \alpha_p \mathbf{g} \end{aligned}$$

total energy balances

$$\begin{aligned} \rho_f \alpha_f (\partial_t + \mathbf{u}_f \cdot \partial_{\mathbf{x}}) E_f + \partial_{\mathbf{x}} \cdot (\alpha_f p_f \mathbf{u}_f + \alpha_p \rho_f \mathbf{r}) + p_f \partial_{\mathbf{x}} \cdot (\alpha_p \mathbf{u}_p) &= D_{pf} + D_E + \rho_f \alpha_f \mathbf{g} \cdot \mathbf{u}_f \\ \rho_p \alpha_p (\partial_t + \mathbf{u}_p \cdot \partial_{\mathbf{x}}) E_p + \partial_{\mathbf{x}} \cdot (p_p \mathbf{u}_p) + \alpha_p \mathbf{u}_p \cdot \partial_{\mathbf{x}} p_f &= D_{fp} - D_E + \rho_p \alpha_p \mathbf{g} \cdot \mathbf{u}_p \end{aligned}$$

where $\alpha_f + \alpha_p = 1$,

$$\begin{aligned} \mathbf{R} &= \frac{1}{5} u_{fp}^2 \mathbf{I} + \frac{2}{5} \mathbf{u}_{fp} \otimes \mathbf{u}_{fp} \quad \mathbf{r} = \mathbf{R} \cdot \mathbf{u}_p + \Theta_p (\mathbf{u}_p + 2\mathbf{u}_{pf}) \quad D_E = K (3\Theta_p + \mathbf{u}_p \cdot \mathbf{u}_{pf}) \\ D_{pf} &= -D_{fp} = \mathbf{u}_p \cdot \mathbf{F}_{pf} + 2\alpha_p \Theta_p [\mathbf{u}_{pf} \cdot \partial_{\mathbf{x}} \rho_f - \rho_f (\partial_{\mathbf{x}} \cdot \mathbf{u}_v) - \rho_f \partial_{\mathbf{x}} \cdot (\alpha_p \mathbf{u}_{fp})] \\ \mathbf{u}_{fp} &= -\mathbf{u}_{pf} = \mathbf{u}_f - \mathbf{u}_p \quad p_f = \rho_f \Theta_f \quad p_p = \rho_p \alpha_p \Theta_p (1 + 4\alpha_p g_0) \quad g_0 = \frac{1 + \alpha_f}{2\alpha_f^3} \\ \Theta_f &= \frac{2}{3} \left(E_f - \frac{1}{2} u_f^2 \right) \quad \Theta_p = \frac{2}{3} \left(E_p - \frac{1}{2} u_p^2 \right) \end{aligned}$$

Table 1. Two-fluid model for flow of an ideal fluid and elastic hard-sphere particles with constant ρ_p . $\mathbf{F}_{pf} = -\mathbf{F}_{fp}$ is given in terms of the pfp-pressure tensor \mathbf{P}_{pfp} and the volume-average velocity $\mathbf{u}_v = \alpha_p \mathbf{u}_p + \alpha_f \mathbf{u}_f$ in (3.5). To include added mass, as done in Fox *et al.* (2020), it suffices to make the following substitutions: $\alpha_p \rightarrow \alpha_p^*$, $\rho_p \rightarrow \rho_e$, $\alpha_f \rightarrow \alpha_f^*$; and to include a mass balance for α_p , as well as the added-mass exchange terms (see Boniou *et al.* 2024 for details). Note that, for clarity, the frictional pressure needed for dense granular flows (see, e.g. Houim & Oran 2016) has not been included in the definition of p_p . With or without added mass, the frictional pressure depends only on α_p .

$$\mathbf{F}_{pf} = \partial_{\mathbf{x}} \cdot \mathbf{P}_{pfp} + \alpha_p \rho_f \frac{4}{5} \mathbf{\Gamma}_v \cdot \mathbf{u}_{fp} + \alpha_p (\Theta_p \mathbf{I} + \alpha_f \mathbf{R}) \cdot \partial_{\mathbf{x}} \rho_f + \alpha_p \rho_f \frac{2}{5} (\partial_{\mathbf{x}} \cdot \mathbf{u}_v) \mathbf{u}_{fp}. \tag{3.5}$$

The first two terms on the right-hand side are present even when ρ_f is constant, in which case the last two are zero. The second term is a lift force due to gradients in \mathbf{u}_v (and not \mathbf{u}_f); however, in the dilute limit $\alpha_p \rightarrow 0$ (i.e. the lift force on a single particle), these two velocities are nearly identical. Alternatively (i.e. using the traceless tensor \mathbf{S}_v as done in Fox 2019), the tensor $\mathbf{\Gamma}_v$ in the lift force can be made traceless and one third its trace combined with the final term in (3.5).

Given that $\mathbf{F}_{fp} = -\mathbf{F}_{pf}$, we can observe that by moving $\partial_{\mathbf{x}} \cdot \mathbf{P}_{pfp}$ to the left-hand sides of the momentum balances in table 1, \mathbf{P}_{pfp} acts like a (positive) pressure term for the particle phase. For the fluid phase, we can combine the \mathbf{P}_{pfp} term with the momentum flux due to \mathbf{R} to find

$$\partial_{\mathbf{x}} \cdot [\alpha_p \rho_f (\Theta_p \mathbf{I} + \mathbf{R})] - \partial_{\mathbf{x}} \cdot \mathbf{P}_{pfp} = \partial_{\mathbf{x}} \cdot [\alpha_p \rho_f (\Theta_p \mathbf{I} + \alpha_f \mathbf{R})], \tag{3.6}$$

and thus the combined term acts as a pressure as well. In agreement with Zhang (2021), this would suggest that a pfp-pressure tensor should be present in every two-fluid model for disperse multiphase flows, regardless of how the model is derived.

4. Discussion and conclusions

4.1. Physical interpretation of \mathbf{F}_{pf}

The force \mathbf{F}_{pf} has two contributions: one due to the fluid-density gradient at constant pressure, and one due to the fluid-velocity gradient. The first is important in high-speed flows with shock waves. At a contact surface behind a shock wave, the fluid pressure is constant but the density gradient is large. Here, \mathbf{F}_{pf} provides an unsteady drag on the particles due to the density gradient (Boniou & Fox 2023). In low-speed flows, the fluid-density gradient is small (or zero), in which case \mathbf{F}_{pf} depends only on fluid-velocity gradients. Physically, when \mathbf{u}_f varies over the length scale $d_p/2$, a hydrodynamic force results. Because $\mathbf{u}_f = \mathbf{u}_v + \alpha_p \mathbf{u}_{pf}$ and (with constant ρ_f) $\partial_{\mathbf{x}} \cdot \mathbf{u}_v = 0$, the hydrodynamic stress scales like $\rho_f \alpha_p^2 u_{pf}^2$ (see Zhang *et al.* 2006; Zhang 2021 for details). Thus, in addition to the fluid-drag force found for uniform \mathbf{u}_f , there is ‘slip stress’ when \mathbf{u}_f varies across the particle radius (i.e. for non-zero $\partial_{\mathbf{x}} \mathbf{u}_f$). Finally, it is important to notice that \mathbf{F}_{pf} does not depend directly on gradients of α_p . This is because at the scale of the particle, α_p is not defined (or constant). Thus, in the kinetic model in (2.1) for an ideal-fluid–particle system, the Enskog contribution to $f^{(2)}$ does not depend on the gradient of f_p . Nonetheless, recent work (Wang, Zhang & Balachandar 2024) has demonstrated that a volume-fraction gradient leads to a diffusion stress Σ_d . The reader is referred to Wang *et al.* (2024) for the exact definition, but it is important to note that such a stress will affect the hyperbolicity of the two-fluid model. Indeed, a similar term is widely used in two-fluid models for bubbly flows to make them well-posed (Lhuillier *et al.* 2013; Panicker *et al.* 2018).

4.2. Is the two-fluid model well-posed?

As shown in Fox *et al.* (2020), since the trace of \mathbf{P}_{pfp} is $\rho_f \alpha_p^2 u_{pf}^2$, the pfp-pressure will be large enough to keep the two-fluid model well posed. For an incompressible fluid (see table 2), the two eigenvalues for the particle phase $\lambda_{1,2} = u_p + u_{fp} \hat{\lambda}_{1,2}$ can be computed analytically (Panicker *et al.* 2018). Subtracting $u_p = 0$ and dividing the result by u_{fp} , we find the two scaled eigenvalues (this result is strongly dependent on using both the correct pfp-pressure and fluid-phase momentum flux. For example, using $\partial_{\mathbf{x}} \cdot \mathbf{P}_{pfp}$ without $\partial_{\mathbf{x}} \cdot [\alpha_p \rho_f (\Theta_p \mathbf{I} + \mathbf{R})]$ yields very different (non-physical) eigenvalues for small Θ_p)

$$\hat{\lambda}_{1,2} = \frac{Z \alpha_p \alpha_f \pm X^{1/2}}{(\alpha_f + Z \alpha_p) \alpha_f}, \quad (4.1)$$

with (if the particle–particle collisions are inelastic with coefficient of restitution e_c , then $p_p = \alpha_p \Theta_p [1 + 2(1 + e_c) \alpha_p g_0]$). The second and third terms on the right-hand side of (4.2) then depend on e_c , but the qualitative behaviour of the eigenvalues remains the same)

$$X = (1 - \hat{\Theta}_p) Z^2 \alpha_p^2 \alpha_f^2 + \frac{2}{\alpha_f} (3 + \alpha_f) \alpha_p^2 Z \hat{\Theta}_p + (\alpha_p^4 + 4 \alpha_f \alpha_p^2 + 4 \alpha_p + 1) \hat{\Theta}_p, \quad (4.2)$$

where $\hat{\Theta}_p = \Theta_p / u_{fp}^2$. As seen in figure 1, these eigenvalues are real and distinct for all α_p when $X > 0$. As only the first term in (4.2) can be negative when $\hat{\Theta}_p > 1$, an ill-posed

$$\begin{aligned} \partial_t \alpha_f + \partial_x (\alpha_f u_f) &= 0 \\ \partial_t \alpha_p + \partial_x (\alpha_p u_p) &= 0 \\ \alpha_f (\partial_t + u_f \partial_x) u_f + \partial_x (\alpha_p \Theta_p) + \partial_x (\alpha_p \alpha_f u_{fp}^2) + \alpha_f \partial_x p_f &= 0 \\ \alpha_p (\partial_t + u_p \partial_x) u_p + \partial_x [\alpha_p \Theta_p (1 + 4\alpha_p g_0)] + Z \partial_x (\alpha_p^2 u_{pf}^2) + Z \alpha_p \partial_x p_f &= 0 \end{aligned}$$

Table 2. One-dimensional two-fluid model with a constant-density fluid and constant granular temperature Θ_p . The source terms are neglected because they do not affect the eigenvalues. The primitive variables are $X = [p_f, \alpha_p, u_p, u_f]$ where the fluid pressure is divided by ρ_f . Two eigenvalues for this system are $\pm\infty$ (Panicker *et al.* 2018), and the other two can be scaled to depend only on Z and $\hat{\Theta}_p$ (Fox *et al.* 2020). In the particle-phase momentum balance, the second term is the granular pressure, the third term is the pfp contribution, while the fourth is due to the Archimedes force. The pfp and $\alpha_p R$ contributions are combined in the fluid-phase momentum balance, yielding a positive ‘slip pressure’ as in (3.6).

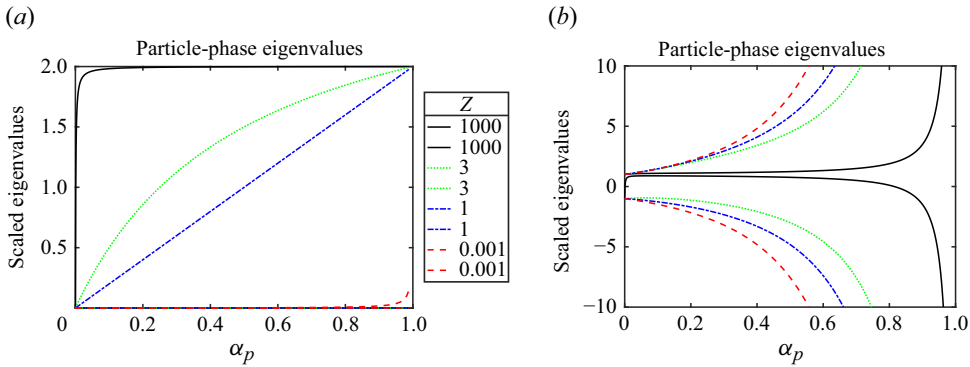


Figure 1. Scaled particle-phase eigenvalues with an incompressible fluid found from (4.1) with (a) $\hat{\Theta}_p = 0$ and (b) $\hat{\Theta}_p = 1$. Lines: solid black, $Z = 1000$; dotted green, $Z = 3$; dash-dot blue, $Z = 1$; dashed red, $Z = 0.001$. With $\hat{\Theta}_p = 0$, one scaled eigenvalue is zero. For larger $\hat{\Theta}_p$, the eigenvalues separate more rapidly with increasing α_p . When added mass is included (Fox *et al.* 2020; Boniou *et al.* 2024), bubbly flow corresponds to $Z \approx 3$, and the eigenvalues are real for all $\hat{\Theta}_p \geq 0$.

system may arise if Z is large enough. In the granular limit, $Z = 0$ and $\hat{\lambda}_{1,2} \propto \pm \hat{\Theta}_p^{1/2}$ as expected, while for massless particles $Z \rightarrow \infty$ and $\hat{\lambda}_{1,2} = 1 \pm (1 - \hat{\Theta}_p)^{1/2}$. However, when added mass is included in the two-fluid model (see Fox *et al.* 2020; Boniou *et al.* 2024 for details), the effective density of the particles ρ_e depends on the added-mass coefficient $C_m \approx 0.5$ (for the two-fluid model with added mass to be well posed for all Θ_p , the minimum value is $C_m \approx 0.1$, which gives $Z \approx 11$ when $\rho_p \rightarrow 0$) such that $Z = \rho_f / \rho_e \leq 3$. In that case, the two eigenvalues are real for all $\hat{\Theta}_p \geq 0$. Likewise, when the frictional pressure is included in the particle-phase pressure p_p , the particle-phase eigenvalues have much larger magnitude when $\alpha_p > 0.63$ (Houim & Oran 2016). We can therefore conclude that the two-fluid model derived in Fox (2019) with the pfp-pressure tensor given in (3.4) and the added-mass model in Fox *et al.* (2020), Boniou *et al.* (2024) is well posed for all physically relevant conditions.

Concerning the physical interpretation of the eigenvalues in figure 1, the results for $\Theta_p = 0$ are of particular interest. In a frame of reference with $u_p = 0$, the particles are fixed with zero mean and fluctuating velocity, and the slip velocity u_{fp} is in the positive direction (e.g. gravitational sedimentation). This results in $\lambda_1 = 0$ so that no information about the particles travels upstream (i.e. ahead of the falling particles). On the other

hand, the wave with $\lambda_2 = 2Z\alpha_p u_{fp}/(\alpha_f + Z\alpha_p)$ will propagate particle-phase mass and momentum downstream at speeds that can exceed the mean fluid velocity for $Z \geq 1$. This will cause a cloud of particles to spread only in the downstream ($u_{fp} > 0$) direction. In most applications (e.g. Boniou & Fox 2023), $0 < \hat{\Theta}_p \ll 1$ so that information propagates in both directions. Nonetheless, due to its dependence on Z , including the pfp-pressure term (and added mass) is crucial for lightweight particles such as bubbles (Risso 2018) or even inertial granular suspensions (Guazzelli & Pouliquen 2018).

In summary, like the Euler equations for ideal-fluid flow, the two-fluid model in table 1 for ideal-fluid–particle flow is the simplest possible model containing the minimum physics needed to be well posed. Thus, it can be used as the starting point for adding more physics such as viscous effects, mass transfer and chemical reacting species (Boniou *et al.* 2024). Unlike the ‘standard’ two-fluid model used in most academic and commercial codes, the model in table 1 has the fluid-phase flux term \mathbf{R} and the pfp-pressure tensor \mathbf{P}_{pfp} , both of which arise (like the Archimedes force) from the excluded volume of the particles. Given this fact, it is reasonable to expect that the fluid–particle model in table 1 can be used as a starting point for other particle shapes besides spheres, albeit with corrections to some of the exchange terms (e.g. the drag coefficient K).

Acknowledgements. The author would like to thank the Massot group at CMAP–École Polytechnique for motivating him to take a fresh look at the relationship between \mathbf{F}_{pf} and \mathbf{P}_{pfp} . The insightful comments and comprehensive feedback from the anonymous referees was highly appreciated by the author and greatly improved the readability and focus of this work.

Funding. For the performance of this research, the author was supported by the Fulbright–Tocqueville Distinguished Scholar and Jean D’Alembert Senior Professor Chair at the Université de Paris-Saclay.

Declaration of interests. The author reports no conflict of interest.

REFERENCES

- VAN BEIJEREN, H. & DORFMAN, J.R. 1980a Kinetic theory of hydrodynamic flows. I. The generalized normal solution method and its application to the drag on a sphere. *J. Stat. Phys.* **23** (3), 335–402.
- VAN BEIJEREN, H. & DORFMAN, J.R. 1980b Kinetic theory of hydrodynamic flows. II. The drag on a sphere and on a cylinder. *J. Stat. Phys.* **23** (4), 443–461.
- BONIOU, V. & FOX, R.O. 2023 Shock–particle-curtain study with a hyperbolic two-fluid model: effect of particle force models. *Intl J. Multiphase Flow* **169**, 104591.
- BONIOU, V., FOX, R.O., POSEY, J.W. & HOUIM, R.W. 2024 A multiphase model for fluid–particle flows with added mass and phase change. *Chem. Engng J.* **502**, 157967.
- CAPECELATRO, J. 2022 Modeling high-speed gas–particle flows relevant to spacecraft landings. *Intl J. Multiphase Flow* **150**, 104008.
- CERCIGNANI, C. 1988 *The Boltzmann Equation and Its Applications*. Springer.
- CHAPMAN, S. & COWLING, T.G. 1952 *The Mathematical Theory of Non-Uniform Gases*. 2nd edn. Cambridge University Press.
- COOK, T.L. & HARLOW, F.H. 1984 Virtual mass in multiphase flow. *Intl J. Multiphase Flow* **10** (6), 691–699.
- DREW, P.A. & PASSMAN, S.L. 1998 *Theory of Multicomponent Fluids*. Springer.
- FOX, R.O. 2019 A kinetic-based hyperbolic two-fluid model for binary hard-sphere collisions. *J. Fluid Mech.* **877**, 282–329.
- FOX, R.O. 2024 Recent advances in well-posed Eulerian models for polydisperse multiphase flows. *Intl J. Multiphase Flow* **172**, 104715.
- FOX, R.O., LAURENT, F. & VIÉ, A. 2020 A hyperbolic two-fluid model for compressible flows with arbitrary material-density ratios. *J. Fluid Mech.* **903**, A5.
- GUAZZELLI, É. & POULIQUEN, O. 2018 Rheology of dense granular suspensions. *J. Fluid Mech.* **852**, P1–1–73.
- HOUIM, R.W. & ORAN, E.S. 2016 A multiphase model for compressible granular–gasous flows: formulation and initial tests. *J. Fluid Mech.* **789**, 166–220.
- LHUILIER, D. 2023 Personal communication.

- LHULLIER, D., CHANG, C.-H. & THEOFANOUS, T.G. 2013 On the quest for a hyperbolic effective-field model of disperse flows. *J. Fluid Mech.* **731**, 184–194.
- MARCHISIO, D.L. & FOX, R.O. 2013 *Computational Models for Polydisperse Particulate and Multiphase Systems*. Cambridge University Press.
- PANICKER, N., PASSALACQUA, A. & FOX, R.O. 2018 On the hyperbolicity of the two-fluid model for gas–liquid flows. *Appl. Math. Model.* **57**, 432–447.
- RISSE, F. 2018 Agitation, mixing, and transfers induced by bubbles. *Annu. Rev. Fluid Mech.* **50** (1), 25–48.
- WANG, M., YANG, Y., ZHANG, D.Z. & BALACHANDAR, S. 2021 Numerical calculation of the particle–fluid–particle stress in random arrays of fixed particles. *Phys. Rev. Fluids* **6** (10), 104306.
- WANG, M., ZHANG, D.Z. & BALACHANDAR, S. 2024 Effect of the volume fraction gradient on the phase interaction force model for disperse two-phase models. *Phys. Rev. Fluids* **9** (10), 104301.
- ZHANG, D.Z. 2021 Ensemble average and nearest particle statistics in disperse multiphase flows. *J. Fluid Mech.* **910** (A16), 1–22.
- ZHANG, D.Z., MA, X. & RAUENZAHN, R.M. 2006 Interspecies stress in momentum equations for dense binary particulate systems. *Phys. Rev. Lett.* **97** (4), 048301.